P2.1 Combined analysis of local downslope wind “Hiroto-kaze” induced by Typhoon “TOKAGE” in Japan

Fumie Kataoka[1*], Y. Mitomi[1], K. Otsuka[2], O. Tsukamoto[3], H. Fudeyasu[4], T. Kanamori[5], T. Kuwagata[6], T. Hashimoto[3], K. Kobayashi[3], and K.Tsuboki[7]

[1]Remote Sensing Technology Center of Japan, Ibaraki, Japan
[2]Technical Research Institute, Obayashi Corporation, Tokyo, Japan
[3]Department of Earth Sciences Okayama University, Okayama, Japan
[4]International Pacific Research Center, University of Hawaii, Honolulu, Hawaii
[5]Kobe Marine Observatory, Hyogo, Japan
[6]National Institute for Agro-Environmental Sciences, Ibaraki, Japan
[7]Hydrospheric-Atmospheric Research Center, Nagoya University, Japan

1. INTRODUCTION

Downslope winds occure when critical combinations of the topographic and the atmospheric conditions are satisfied. "Hiroto-kaze” is one of the strongest local donwslope winds in Japan, which blows on the south foot of Mt. Nagi (1250m) located in the north-eastern part of Okayama prefecture (Figure.1). It causes damage of crops and constructions in Nagi area. Accordingly, it is a traditional landscape that many houses have tree fences on their north faces.

Figure 2 show a topographic map focused on Mt.Nagi. The topography of Mt.Nagi is characterized by smooth but steep slope of its southern foot, which is contrasted with rather gentle and mountainous features of north foot. And on the north side of Mt.Nagi, Sendai River valley runs to the Japan Sea. These conditions enforce the southward airflow to converge both vertically and horizontally.

In 2004, two major "Hiroto-kaze" events were observed. The one accompanied by Typhoon MEARI was a typical "Hiroto-kaze", while the other associated with Typhoon TOKAGE was super "Hiroto-kaze" in magnitude and the extent of wind-damage area. In the latter case, extensive damage of fallen trees spread over the northern Okayama prefecture. The amount of damage totaled to be more than 6.5 billion yen.

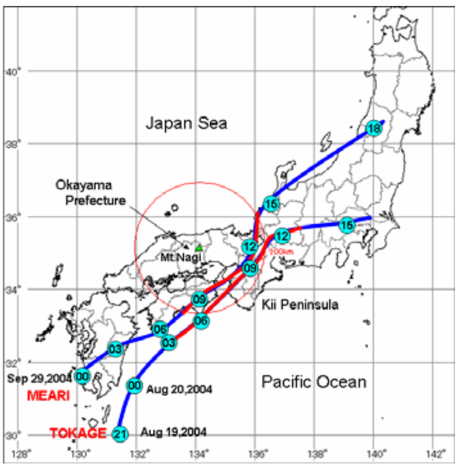

Figure.1. Track of typhoon MEARI and TOKAGE. Typhoon center is indicated at every 3-h.Red line shows the position of typhoon when “Hiroto-kaze” occurred.

----

* *Corresponding author address:* Fumie Kataoka, Remote Sensing Technology Center of Japan, Tsukuba-Mitsui BLDG 18F, 1-6-1 Takezono, Tsukuba-city, Ibaraki, 305-0032, JAPAN ; e-mail: kataoka.fumie@restec.or.jp.

2. OBSERVATIONAL CASE STUDIES OF "Hiroto-kaze"

In this study, we investigate two cases of “Hiroto-kaze" as follows. One is accompanied by typhoon MEARI, the other is by typhoon TOKAGE. As shown in Figure 1, these typhoons treated a similar course, but the latter induced one was the most powerful in resent 50 years.

“Hiroto-kaze” continues to blow when the typhoons or cyclones are passing within a few hundred kilometers south or southeast of Mt. Nagi like Kii peninsula area (indicated by red circle in Figure 1).

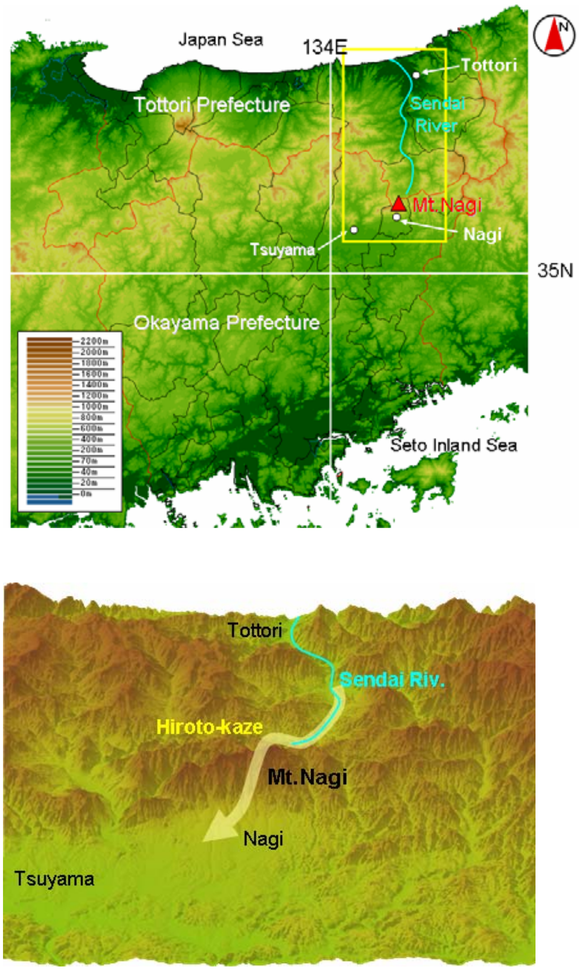

Figure.2. Topographic feature of Okayama and Tottori Prefecture (above). Below shows the birds-eye view focusing yellow rectangle of above figure and schematic flow of “Hiroto-kaze”.

2.1 *TYPHOON MEARI (TYPICAL “Hiroto-kaze”)*

Typhoon MEARI moved northeastward crossing Japan on September 29, 2004. At 0900UTC when the typhoon made landfall on Shikoku Island, the central atmospheric pressure was 980 hPa. When the typhoon entered within 200km radius from Mt.Nagi, the wind became strong rapidly around Nagi area as shown in Figure 3(a). This is what is called “Hiroto-kaze”. At the same time, a drastic change of the wind direction from south to north was observed on the summit of Mt.Nagi. Then strong wind continued for about six hours and the maximum wind speed of 42ms^{-1} was recorded at Nagi at about 1030UTC.On the other hand, in Tsuyama, which located several kilometers west of Nagi town, the wind was not so strong. This means that, in typical "Hiroto-kaze" events, the occurrence of strong wind is rather restricted within the area around Nagi town.

Additionally, a large temperature drop of about 5 degrees in precedent to the onset of strong wind was observed. That is one of the characteristics of the so called “Bora type” topographically induced local winds.

2.2 *TYPHOON TOKAGE (SUPER “Hiroto-kaze”)*

Typhoon TOKAGE followed the similar track to MEARI. But it was significantly larger in size than MEARI.

Since the time when TOKAGE made landfall on Shikoku Island with a central atmospheric pressure of 950 hPa at about 0300UTC October 20 2004, when TOKAGE had still kept the strong wind and rainfall, the wind blew up gradually at Nagi as shown in Figure 3(b).And the maximum wind speed of 51.8ms^{-1} was observed at about 0800UTC. In different to the case of MEARI, the maximum gust of 50.3ms^{-1} was recorded at Tsuyama, where wind was mostly rather moderate, at the same time. Throughout the period of more than half a day, the strong wind had been blowing.

As shown in Figure 4, it is noted that the pressures at Nagi and Tsuyama are clearly lower than the general features of the parabolic variation of the surface pressure with the distance from the center of a typhoon. The local pressure minima at these sites are the signs of the occurrences of downslope wind and subsequent damages. So we will investigate the distribution of wind damage using satellite data.

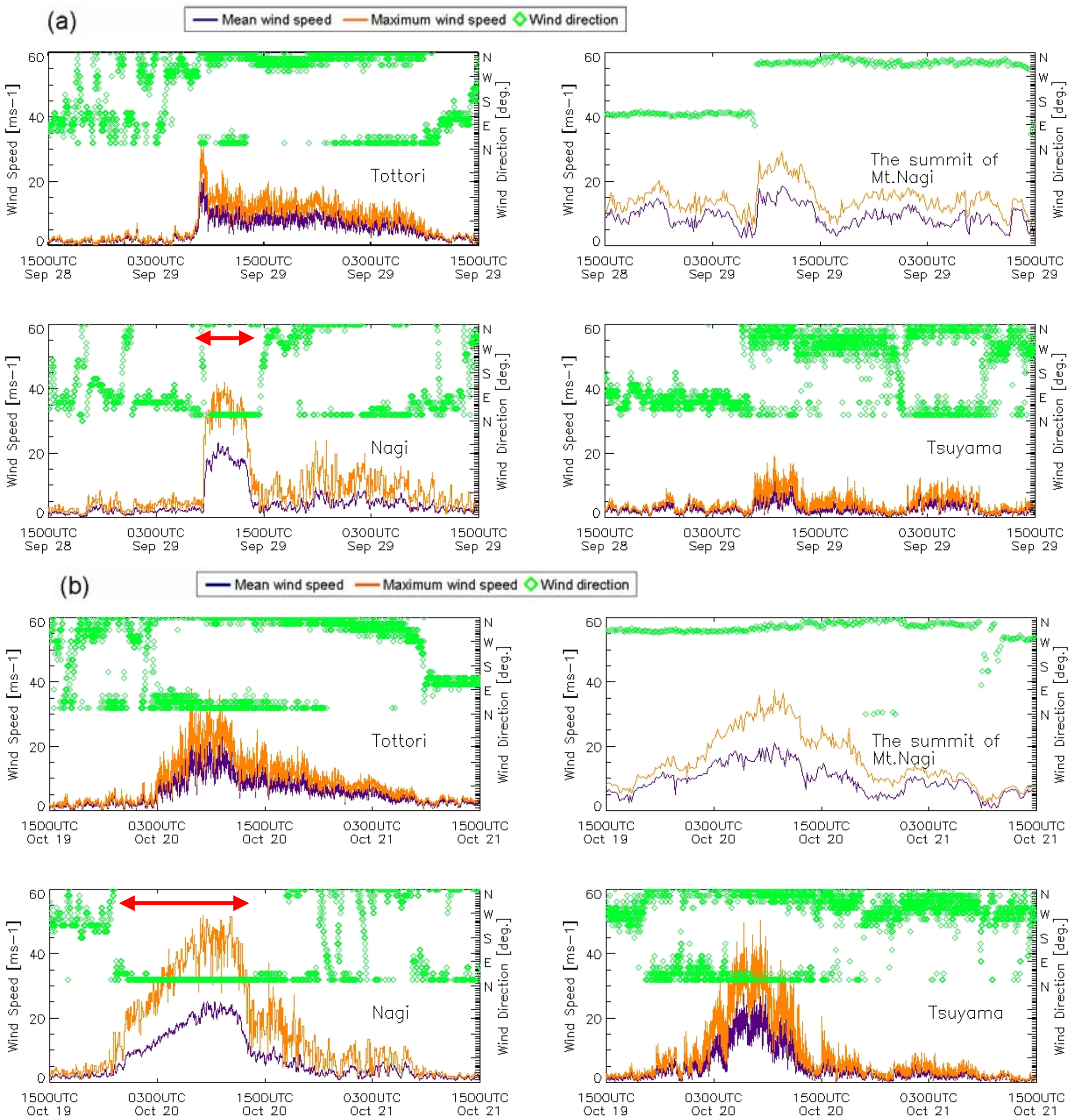

Figure.3. Time series of the wind speed (lines) and the wind direction (dots) at each meteorological station during the period of (a) MEARI and (b) TOKAGE. Red arrows indicate the period of “Hiroto-kaze”.

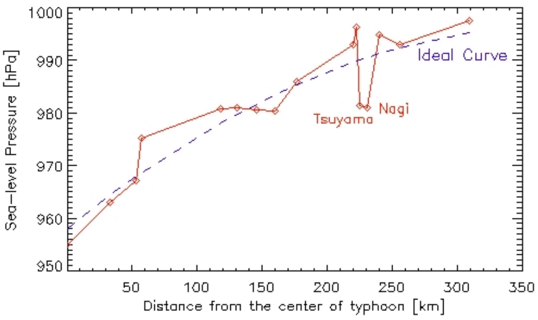

Figure.4. Radial distribution of sea level pressure on 0600UTC October 20 2004 (solid line) and ideal curve of pressure (broken line).

3. EXTRACTION OF FALLEN TREES AREA USING SATELLITE DATA

To obtain fallen tree areas, we used ASTER data which provide high spatial resolution and hyper-spectral images. ASTER, stands for Advanced Space borne Thermal Emission and Reflection Radiometer and is onboard the NASA EOS Terra satellite platform, launched into sun-synchronous Earth orbit on December 18 ,1999, and started sending data back to the earth in February 2000.It covers a wide spectral region from the visible to the thermal infrared by 14 spectral bands (VNIR, SWIR, TIR). This time, we focused on VNIR spectral data shown in Table 1.

The following clear-day data are chosen for the comparison of the images between before and after the strong wind events on October 20, 2004.

- Before event : May 21,2003 (0158UTC)
- After event : June 20,2005 (0151UTC)

TABLE.1. Characteristics of the ASTER VNIR bands.

Band No.	*Spectral Range [μm]*	*Spatial Resolution[m]*
1	0.52-0.60	15
2	0.63-0.69	15
3N	0.78-0.86	15
3B	0.78-0.86	15

3.1 *PREPARATION OF SATELLITE DATA*

Before analyzing the satellite data, we executed the following data processing.

3.1.1 *RADIOMETRIC CONVERSION*

The ASTER Level-1B data are offered in terms of scaled radiance. In order to convert from DN to radiance at the sensor, the unit conversion coefficients (defined as radiance per 1 DN) are used. Radiance (spectral radiance), which expressed in unit of W/(m^2*sr*μm), can be obtained from DN values as follows.

Radiance = (DN value – 1) x Unit conversion coefficient (1)

In order to directly compare hyper-spectral image with reference reflectance spectra, the encoded radiance values in the image must be converted to reflectance. A comprehensive conversion must account for the solar source spectrum, lighting effects due to sun angle and the characteristics of the sensor system. So we derived the reflectance from following equations.

$$\rho = \frac{\pi \cdot L}{F_0 \cdot \cos\theta} \quad , \tag{2}$$

where ρ is the reflectance , L is the radiance , F_0 is the extraterrestrial Solar Spectral Irradiance from World Radiation Center (WRC) table which was used in ASTER calibration work ,and $\cos\theta$ is the solar zenith angle (zenith angle = 90 – solar elevation angle). When we employ the solar irradiances, we have been weight-integrated the WRC solar spectral irradiance by spectral responses of every ASTER bands shown in Figure 5.

$$F(b) = \sum_{\lambda=l_1}^{l_2} \{E_0(\lambda)\cdot\Psi_b(\lambda)\} / \sum_{\lambda=l_1}^{l_2} \Psi_b(\lambda), \tag{3}$$

where F(b) is the ASTER band weighted solar irradiance, E_0 is WRC solar spectral irradiance table,Ψ is ASTER spectral response for band b, l1 and l2 are the minimum and the maximum wavelength λ where both the ASTER response and WRC solar irradiance are available.

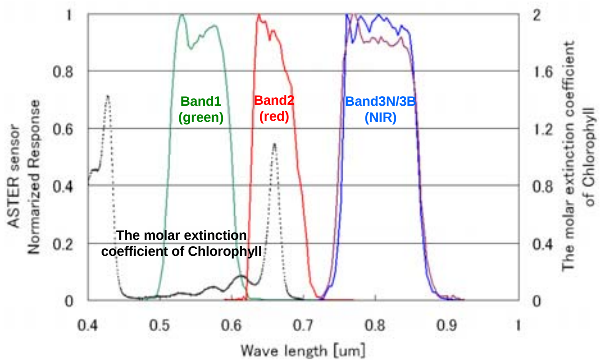

Figure.5. Normalized spectral response curves of ASTER VNIR (1, 2, and 3N/B) and the molar extinction coefficient of Chlorophyll.

3.1.2 *GEOMETRIC CONVERSION*

The ASTER Level-1B data have a geometric correction table which contains the latitude and the longitude values at lattice points and can be extracted from the HDF file. The latitude and the longitude values at other pixel position can be calculated by linear interpolation from the values at the lattice points. The latitude values are expressed as the geocentric coordinates. The geocentric latitude α can be easily converted into the geodetic latitude β.

$$\tan\beta = C \cdot \tan\alpha$$
$$C = 1.0067395 \tag{4}$$

This time, we used two season data sets, which were observed on different day. For comparing these data with the spectral, we applied a precise geometric correction, the affine transformation and the third-order polynomial interpolation using Ground Control Points (GCPs).

3.2 *ANALYSIS OF SATELLITE DATA*

3.2.1 *EXTRACTION OF FALLEN TREES AREA*

In fallen tree areas, it is expected that trees are losing their containing water and the leaves are dying at the same time, resulting in the reduction of the concentration of leaf chlorophyll and the spectral absorption of solar radiation of the wavelengths corresponding to the absorption bands of chlorophyll. As shown in Figure 5, the molar extinction coefficient of Chlorophyll is high in the red band (band2), so the fallen tree area has higher reflectance than the living forest in the red band. In accordance with these principles, we superimposed the images and extracted the fallen tree areas.

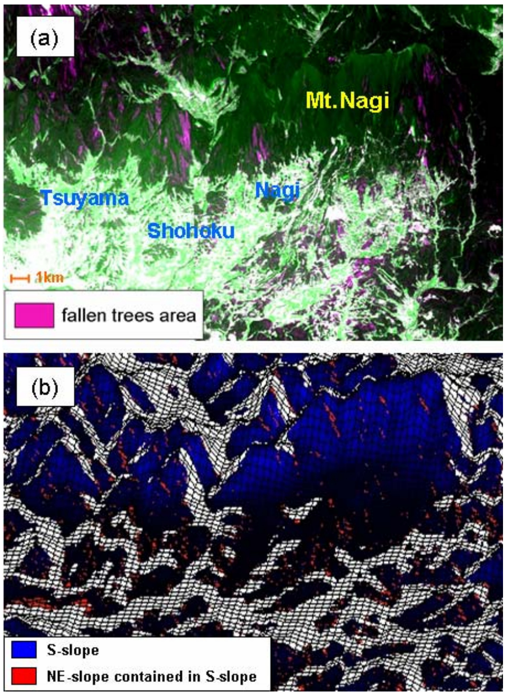

Figure.6. (a) Bird's eyes view of ASTER data near the Mt.Nagi which emphasizes the fallen trees area. (b) Bird's eyes view of elevation data.

Figure 6(a) shows the bird's eyes view of analyzed ASTER data. The fallen tree areas are indicated in pink polygon, which reveal that the damage areas extend not only overt the slope but also over the plane on the south foot of Mt. Nagi.

Alternatively we analyzed how the distribution of the fallen-tree areas related to the topography using digital elevation data. As shown in Figure 6(b), the damage area mainly extended in the south-slope, especially northeastern-slope contained in the south-slope. In Tsuyama, a good deal of damage was done to these slope, it was estimated that northeastern-wind had been blown.

3.2.2 *VALIDATION WITH IN-SITU DATA*

In order to verify the accuracy of analysis, we compare the analyzed satellite data with the field investigation (exploratory investigation and aerial photographs) carried out by the Nagi town office. Figure 7 shows two images focused on Nagi. These results show good agreement between them.

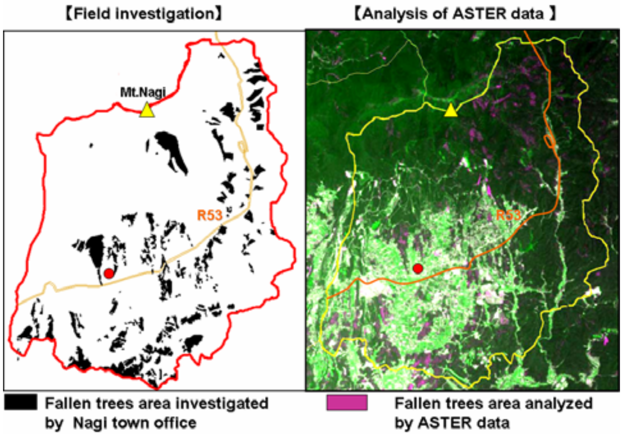

Figure.7. Fallen trees area with in-situ investigated by the Nagi town office (left), and analyzed by ASTER data (right).

4. NUMERICAL SIMULATION

4.1 *MODEL CONFIGURATION*

In order to see the relationship between the fallen tree distribution and meteorological field (typhoon TOKAGE case), numerical model simulation are performed. The numerical simulation results presented in this paper is based on the simulation with CReSS (Cloud Resolving Storm Simulator). It is a non-hydrostatic meteorological model developed by Hydrospheric Atmospheric Research Center, Nagoya University (Tsuboki and Sakaibara, 2005).

The model was run for thirty hours, starting at 1200UTC October 19 2004, with following specifications. The initial and lateral boundary data were provided from output produced by the Regional Spectral Model (RSM: a hydrostatic model used operationally in Japan Meteorological Agency).

Table.2. Specification of numerical simulation

Domain	x 1536 km, y 1408 km, z 18 km
grid number	x 1539, y 1411, z 63
grid size	H 1000m, V 200 ~300m
integration time	30 hrs
ES node numbers	128 nodes (1024 CPUs)

4.2 *RESULTS*

Figure 8(a) shows the topography of simulation domain and figure 8(b) is the distribution of wind speed at 0800UTC October 20. It is apparent that the region of strong wind extends over on the south foot of Mt. Nagi. Tsuyama also shows a pattern of the spread of strong winds area along terrain. The distributions of the strong wind area well correspond to that of fallen trees.

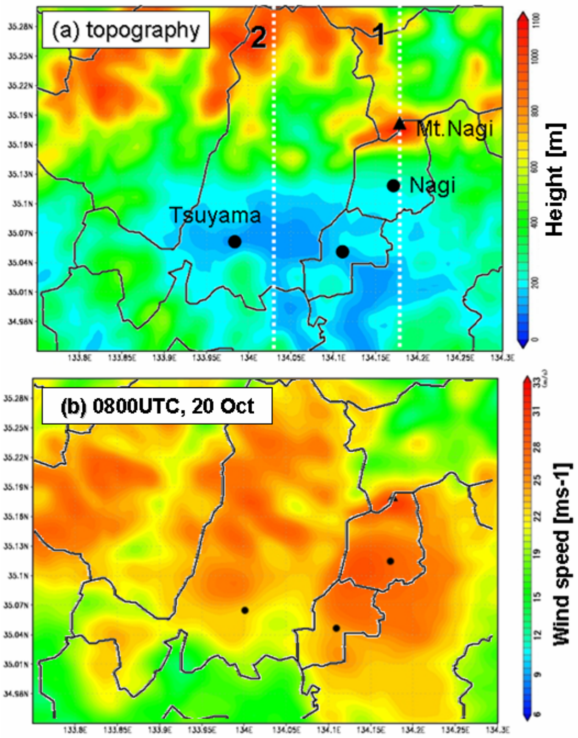

Figure.8. (a) Terrain of simulation domain and (b) distribution of wind speed (0800UTC, 20 Oct 2004).

5. DISCUSSION

The Japan Meteorological Agency (JMA) started the operation of a wind profiler network, the Wind profiler Network and Data Acquisition System (WINDAS), in April 2001. The WINDAS is a network consisting of thirty-one 1.3 GHz-band wind profilers, with spatial resolution of 130km on average over the main islands of Japan. The profiler measures the low level wind field above the sites up to 3000-5000m with an average vertical resolution of 300m.

Figure 9 shows wind profiler data at Tottori for the case of “Hiroto-kaze” events treated here. The Tottori wind profiler is located to the north of Mt.Nagi, so it is considered to approximately give the atmospheric flow conditions upstream of Mt. Nagi. It is noted that, during the period of "Hiroto-kaze", reversal of wind directions (wind shear layer), where the southerly wind is embedded on the three to four kilometer thick northerly wind, is maintained. The height of wind shear gradually rises and when the shear goes over the height of Mt.Nagi, “Hiroto-kaze” starts (Kataoka et al., 2004). As intense cyclones or typhoon pass away the Kii peninsula, the shear layer which acts as mean-state critical layers begin to weaken, resulting on the termination of “Hiroto-kaze”. (Fudeyasu et al., 2008). The wind shear plays an important role in formation of “Hitoro-kaze”. These conditions are satisfied in the case of MEARI as shown in Figure 9(a). This is what is called a typical case. However, the event of associated with TOKAGE is not the case. The wind shear had already existed above the height of Mt.Nagi before the occurrence of “Hiroto-kaze”. And the strong wind had been blowing, even after the shear became ambiguous due to the intrusions of westerly wind. It will be due to the following reasons.

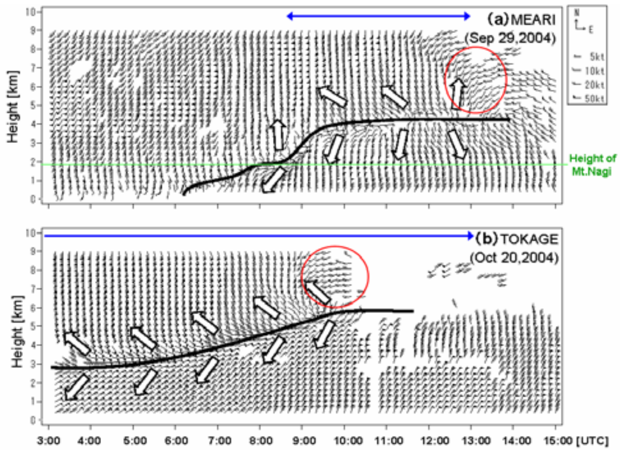

Figure.9. Time series of wind speed and wind direction around “Hiroto-kaze” period (a) MEARI and (b) TOKAGE. Black heavy line indicates shears, white arrows are typical wind direction and blue arrows are period of “Hiroto-kaze”.

First, the rather unusual aspects in the time evolution of the TOKAGE event may be concerned with the size and the structure of the typhoon. Generally, the wind speed within a typhoon is stronger on the right side than the left side relative to the direction of its movement. But the storm relative wind in typhoon TOKAGE was stronger on the left side. There are a number of reports of wind-induced damages caused by the passage of typhoon TOKAGE. Fujibe et al. (2008) reported that TOKAGE was accompanied by the peak gusts exceeding 50ms^{-1} at some stations to the left of the track and located to be more than 100 km.

Second, it will be concerned with the dynamics of mountain waves. The linear theory suggests that the nature of the mountain wave response is characterized by the combinations of the size and the shape of ridge, and the structure of the air flows expressed, for example, by thee vertical distribution of Scorer parameter,

$$l^2 = \left(\frac{N}{U}\right)^2 - \left(\frac{1}{U}\right)\frac{d^2U}{dz^2} \quad , \qquad (5)$$

where, N is the Brunt-Väisälä frequency, U is the mean cross mountain wind speed, and z the vertical coordinate. When l^2 decreases with height, one or more resonant waves can develop in the lower atmosphere in the lee of the mountain. They are called trapped lee waves, which extend downstream from the ridge of crest and produce destructive surface winds (Durran and Klemp, 1982). We calculated the vertical distribution of Scorer parameter using Yonago (near Tottori) upper-air sounding, where the Brunt-Väisälä frequencies averaged over the layers above and below the wind shear.

Figure10 denotes the profiles of wind speed, wind direction and the Scorer parameter at around peak of “Hiroto-kaze”. At 0600UTC October 20 2004, low-level wind direction was northerly, conversely, upper level was southerly. There was a clear shear in middle troposphere. And at 1200UTC, the shear would be ambiguous and the Scorer parameter decrease with height.

Figure 11 shows the vertical cross sections of the potential temperature along the dashed lines in Figure 8(a). Line1 denote Mt.Nagi－Nagi town section and Line2 is Tsuyama section. At 0800UTC, streamlines in both sections move downslope over the southern slope of mountain. This situation will be corresponding to the high-drag transitional flow state. Since there exist wind-induced damage over slope, the wind around Tsuyama will also be "downslope" in nature. At 1200UTC, when the Scorer parameter l^2 decreases with height, wave like streamline are found in leeside of mountain. The propagation of lee wave is considered to have brought about the extensive damages area and sustained strong winds.

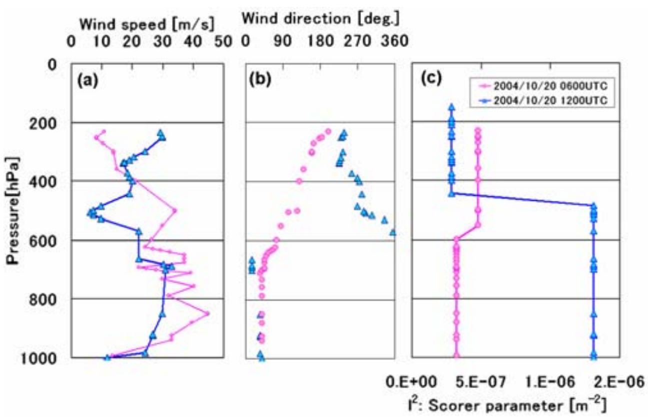

Figure.10. Profiles of (a) wind speed, (b) wind direction and (c) Scorer parameter at 0600UTC, 20 Oct 2004 and 1200UTC, 20 October 2004.

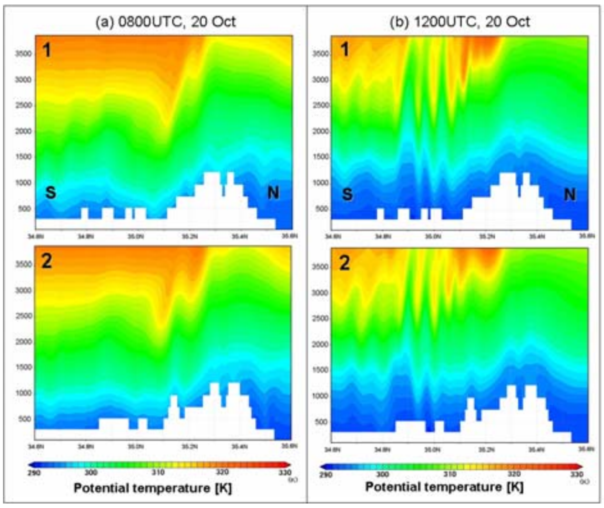

Figure.11. Vertical cross sections of potential temperature at (a) 0800UTC, 20 Oct. (b) 1200UTC, 20 Oct, corresponding to meridian lines1 and 2 in Figure 8(a).

6. SUMMARY

In this study, we analyzed a case of super "Hiroto-kaze" accompanied by Typhoon TOKAGE focusing on relationships between the fallen tree areas and wind field. We were able to extract damage area from ASTER data, especially with the use of red band. The fallen tree distributions derived from the satellite data were consistent not only with the field investigations but also with the simulated surface wind distributions. Alternatively, the wind damage area spread over not only Nagi but also southwestern area like Tsuyama. Usually, "Hiroto-kaze" is confined to Nagi area, but the new maximum wind speed was recorded at Tsuyama in this case. Numerical simulations with the meso-scale model CReSS indicate it possible that a high-drag state downslope wind occurred at that time.

"Hiroto-kaze" induced by two typhoons, which followed similar track, show different behaviors in their onsets and terminations. Typhoon MEARI was, so to speak, a typical one, while the case of typhoon TOKAGE was rather exceptional. In the latter case, strong wind was continuously-blowing even after the shear became ambiguous. This is expected to be due to the following two reasons. The characteristic structure of TOKAGE, in having strong wind in its left sector, is considered to be favorable for the development of the downslope wind in the high-drag state.

Acknowledgements.

The authors would like to thank the Nagi town office for providing exploratory investigation data and aerial photographs.

REFERENCES

Fudeyasu, H., Kuwagata, T., Ohashi, Y., Suzuki, S.i., Kiyohara, Y. and Hozumi, Y., 2008: Numerical Study of the Local Downslope Wind "Hirodo-Kaze" in Japan. , *Mon. Wea. Rev*., **136,** 27–40.

Fujibe, F. and Kitabatake, N. ,2008: Classification of Surface Wind Fields of Tropical Cyclones at Landfall on the Japan Main Islands, *J. Meteor. Soc. Japan*, **85**, 747-765.

Durran, D. R., and J. B. Klemp, 1982: The effects of moisture on trapped mountain lee waves., *J. Atmos. Sci.,* **39,** 2490–2506.

Satomura, T. and Bougeault, P., 1994: Numerical simulation of lee-wave events over the Pyrenees., *J. Meteor. Soc. Japan*, **72**, 173-195

Clark, T. L., and W. R. Peltier, 1984: Critical level reflection and the resonant growth of nonlinear mountain waves., *J. Atmos. Sci.,* **41,** 3122–3134.

Fujibe, F., Kitabatake, H., K. Bessho, and Hoshino, S., 2006: Comparison of surface-wind fields between Typhoon 0418 (Songda) and Typhoon 9119 (Mireille) in western Japan., *Pap. Meteorol. Geophys*. **57**. 1-9.

Nakamura, M., Joko, M., Tsukamoto, O., Kanamori, T., Azuma, K., Kawata ,K., Kimura, H., Kamei, N., Kamata, T. and Fudeyasu, H., 2002: Experimental study of the downslope wind "Hiroto-Kaze" ccurrence at Mt. Nagi (in Japanese). *Tenki,* **49,** 129–139.

Saito,K.,1992: Shallow water flow having a lee hydraulic jump over a mountain range in a channel of variable width., *J. Meteor. Soc. Japan*, **70,** 775-782.

Fujii, T. ,2006: On a pressure distribution of typhoons having made landfall on the Japanese main islands in 2004., *J.JSNDS*, **25-3**, 317-328.

Kitabatake, N . and Bessho, K ., 2008: Cyclone phase of tropical cyclones landfalling in Japan during 2004–2006., *SOLA* , **4**, 21-24.

Doyle,J.D. and Durran, D. R.,2001: The dynamics of mountain-wave-induced rotors, *J. Atmos. Sci.,* **59,** 183–201.

Tsuboki, K., Sakakibara, A., 2005:High-resolution numerical experiments of typhoon using the cloud-resolving model on the Earth Simulator., Proc. of The 7th International workshop on Next Generation Climate Models for Advanced High Performance Computing Facilities, the Second Workshop of "Kyosei" project, Hawaii, U.S.A., pp.38 - 40.

Sasaki.K., Kanno,H., Yokoyama,K., Yokoyama,K.,Matsusima,D.,Moriyama,M.,Fukabori, K. and SHA,W.,2004: Observational evidence of the spatial distribution of wind speed and the vertical structure of the local easterly strong wind "Kiyokawa-dashi" on the Shonai lain, Yamagata.,*Tenki*,**51**, 881-894.